2014 IEEE International Conference on Robotics & Automation (ICRA)
Hong Kong Convention and Exhibition Center
May 31 - June 7, 2014. Hong Kong, China

Simplifying Grasping Complexity through Generalization of Kinaesthetically Learned Synergies

Giuseppe Cotugno[1], Vishawanathan Mohan[2], Kaspar Althoefer[1], Thrishantha Nanayakkara[1]

***Abstract*— There has been a growing enthusiasm to use anthropomorphic hands of humanoid robots to manipulate every-day objects and tools designed for humans. However, multi-fingered grasping imposes a formidable control challenge due to the high dimensionality of the joint space and the difficulty to form a functional grip on objects. We propose a hybrid technique based on grasping synergies extracted from kinaesthetic demonstrations on a given object with a primitive geometry - a cuboid in this case - and passive kinematic enveloping as a generalization technique. Experiments were carried out on an iCub humanoid robot using everyday objects such as a telephone receiver, a computer mouse, three white board markers bundled together, a fencing handle, a compact disc keep case, and a drinking glass. We prove that the primitives extracted from kinaesthetic demonstrations on a cuboid can be generalized across a majority of the above real world objects.**

I. INTRODUCTION

Recently, grasping based on synergies has attracted a lot of enthusiasm among the robotics research community [1]. Neuroscientific studies on human grasping have demonstrated that the brain does not control the motion of the digits individually, but rather as a whole [2], due to the very high number of degrees of freedom (DoF) of the human hand (23 in the simple model of [3]). In other words, the human brain seems to solve the redundancy resolution problem by commanding a group of muscles through combination of a fixed set of muscles synergies that are arranging the digits in a suitable grasping posture. This concept can be modelled mathematically through decomposing a given hand posture into principal components using Principal Component Analysis (PCA). If applied to a human hand joint configuration it is possible to extract a set of *primitives* or *synergies*, each one represented by a different eigenvector (*eigenposture*). Different primitives have a stronger or weaker role in describing the final posture. This feature is expressed by the magnitude of their associated eigenvalue - the higher the value is, the more important the eigenposture is. Authors in [4] have suggested that two or three synergies are sufficient for describing a grasping posture in humans, while adding more primitives in the reconstruction accounts for finer details related to the object. Force applied on the object by each finger can also be taken in consideration during grasping [5].

[1]Giuseppe Cotugno, Kaspar Althoefer, Thrishantha Nanayakkara are with the Centre for Robotics Research, School of Natural and Mathematical Sciences, King's College London, Strand, WC2R 2LS, London, United Kingdom `[giuseppe.cotugno, k.althoefer, thrish.antha] at kcl.ac.uk`

[2]Vishwanathan Mohan is with the Robotics, Brain and Cognitive Sciences Department, Istituto Italiano di Tecnologia, Via Morego 30, 16163, Genoa, Italy `vishwanathan.mohan at iit.it`

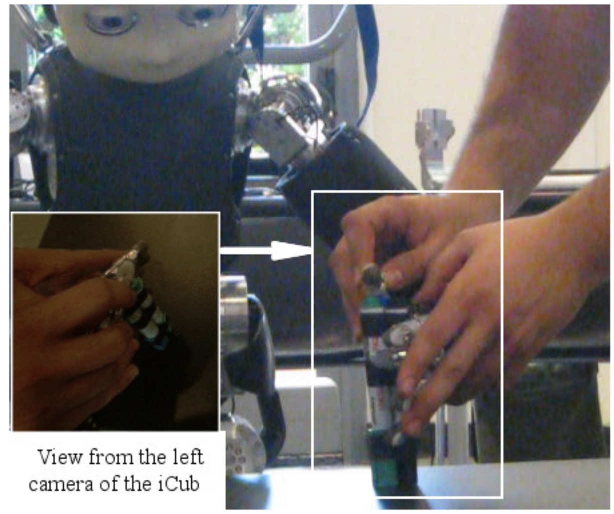

Fig. 1. The iCub kinaesthetically learns to grasp three markers bundled together while the left camera of the robot is recording the scene.

The original approach described in [2], does not take into account the evolution of postures over time. To solve this problem, Singular Value Decomposition (SVD) has been performed on the human motion data while grasping real objects to extract eigenpostures, eigenvalues, and time modulation vectors [6]. Such vectors are explaining how each posture evolves over time offering temporal information on the role of each synergy in grasping.

Mechanical implementations of grasping synergies have been extensively studied in robotics. Notable extension of the initial implementations [7] are soft synergies [8] and adaptive synergies [9]. Regardless of the design choices for the hardware, a hand structurally designed to implement a particular model of synergies is difficult to revert to alternative control strategies without additional complexity in the hardware [10].

Synergies can also be implemented at software level, without the need of customizing hardware. In this case, the robot can learn such postures from human demonstrations executed in a way that enables future grasp analysis. Learning from human demonstrations is a topic that has attracted attention in the past. It is possible to perform demonstrations in many different ways. Some are intrinsic to the robot joint space - e.g. tele-operation or kinaesthetic teaching. Others rely on observing extrinsic data provided by the motion of an external body - e.g. motion capture or observational learning [11]. Furthermore, the collected data must be fitted into a suitable model in order to ensure theirs repeatability, such as dynamic motion primitives [12]. For a more detailed

978-1-4799-3684-7/14/$31.00 ©2014 IEEE

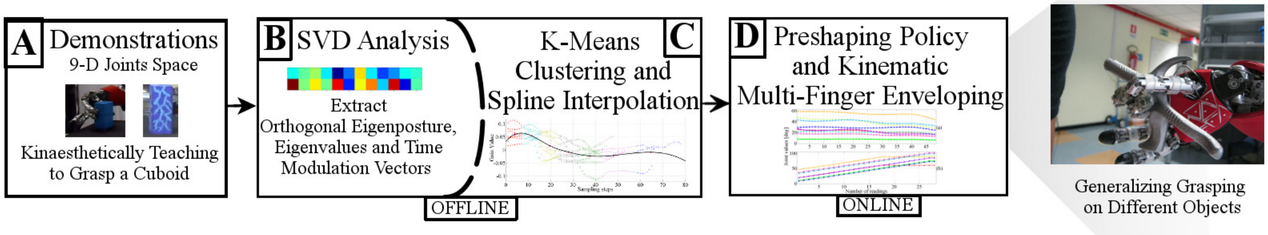

Fig. 2. Summary of the grasping algorithm. [A] Kinaesthetic demonstrations are collected from the joints of the robot. [B] De-noised data are decomposed in orthogonal primitives, eigenvalues and time modulation vectors through SVD. [C] Time modulation vectors from different demonstrations are combined through K-Means and spline interpolation. [D] The preshaping policy resulting from [B] and [C] is executed; Kinematic Enveloping is performed.

description of learning from demonstrations and its features, the reader is referred to [13].

An example of learning from demonstration applied to grasping synergies can be found in [14]. This approach relies on motion capture of human actions. Since the human body is more complex than robot kinematics, there is a substantial kinematic mismatch between the body of the teacher and the one of the robot. This problem is called the *correspondence problem* [15], and it is not trivial to compensate for such discrepancy. The reported technique employ PCA as a decomposition approach. This mathematical method is well established but it cannot take into account the postural variability during the demonstration time line.

In this paper, we present a novel software implementation of grasping synergies based on SVD [16] extracted from kinaesthetic demonstrations. The algorithm benefits from a technique that combines different demonstrations using K-Means clustering and spline interpolation. To improve the generalization ability of the synergies, a technique to dynamically adjust the digits placement on different geometries is illustrated (*kinematic enveloping phase*). The aim of this work is to find and explore answers in response to the following scientific questions: 1) to what extent the proposed method handles the inherent variability in the kinaesthetic demonstrations, 2) how well do the synergies extracted from demonstrations generalize on different objects, 3) how much the enveloping phase can help generalizing the posture, and 4) which part of the grasping algorithm has more impact on the performance.

II. Learning Grasping Synergies from Demonstrations

Since the focus of this work is on grasping, only the 9-finger joints are considered for the analysis. Reaching and wrist orientation alignment is performed by the Passive Motion Paradigm algorithm (PMP) [17].

A. Kinaesthetic Teaching Setup

Experimental data of kinaesthetic teaching were collected from joint encoders in the arm (7 joints) and fingers (9 joints), contact sensors at the fingertips, and visual information from the two cameras as illustrated in Fig. 2.A. Kinaesthetic teaching was performed by a human operator standing next to the robot. In each demonstration trial, the operator held the hands of the robot with the motors switched off, and guided them to perform a pick and place operation. Objects were placed within an easily reachable workspace of the robot.

The nine joints in the robot's hand were organized as follows: one joint controlling adduction/abduction of the digits, three joints for the thumb, two for the index and middle fingers and one for the ring and pinky fingers whose motion is coupled. Each demonstration trial had a minimum of 96 to a maximum of 156 data samples. In total eight trials were performed on pick and place of a cuboid as a primitive object.

B. Extraction of Synergies from Demonstrations

1) Data Preprocessing: The data recorded from the joints of the hand have two trails of redundant stationary data during reaching towards the object and during retration to the home position. These redundnt data were automatically removed using contact initiation and termination of the tactile sensors, in order to make the postural primitives accurately represent the dynamic range of the grasping behavior. Then we used a 3rd order Savitzky-Golay filter [18] with frame size equal to 9 to remove high frequency artefacts in the raw joint data generating an $N \times M$ joint matrix J of preprocessed data. In this case, $N = 9$ was the number of joints in the hand, and $M \in [96, 97, 98, \cdots, 156]$ was the number of data samples in each demonstration trial.

2) Calculation of Synergies: This step is illustrated in Fig. 2.B. Here, singular value decomposition was performed on the preprocessed joint data in J in order to obtain three matrices as given by

$$J = USV^T \tag{1}$$

where U is the $N \times N$ matrix of the eigenpostures, S is the $N \times M$ matrix of the eigenvalues, and V is the $M \times M$ matrix of the temporal modulation coefficients for each primitive in U. In this context, matrix U represents N orthogonal postural primitives of the hand that span the variability of the corresponding grasping demonstration. Each element in the diagonal matrix S represents the significance of the corresponding postural primitive. The higher the values, the more the eigenposture contributes to the variability of the digits. The columns v_i in matrix V represent the scale of temporal modulation of corresponding primitives in U.

In order to decide how many primitives to consider in the analysis, the Root Mean Squared Error (RMSE) is evaluated.

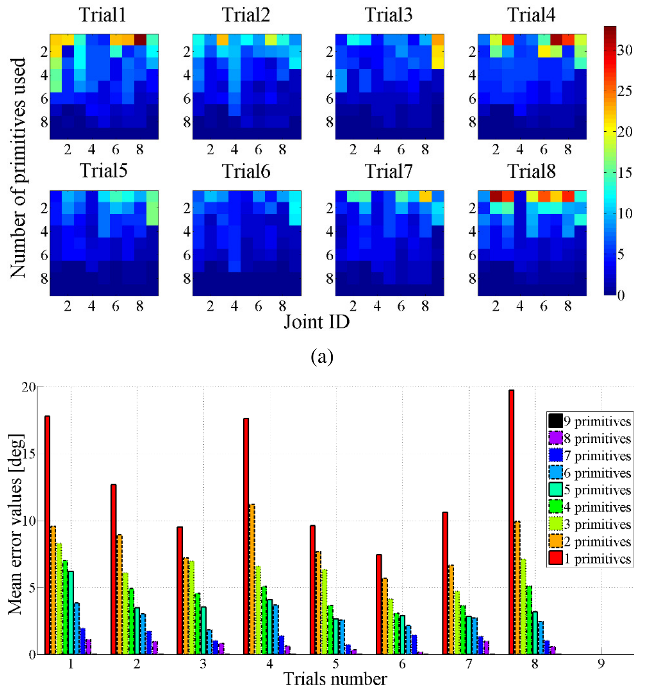

(a)

(b)

Fig. 3. Fig. 3(a) are RMS errors per trial. Each column shows the error on a single joint, while each row shows the error using a different number of primitives (from 1 to 9). Tables have been normalized to 35% to improve visualization. Fig. 3(b) shows the distribution of mean RMS errors using a different number of primitives.

The RMSE for each trial i is calculated for $k = 1, 2, \cdots, 9$ primitives as given by

$$RMSE_i^{(k)} = \sqrt{\frac{[(U^{(k)} S^{(k)} V^{(k)^T}) - J]^2}{M}}, \tag{2}$$

where $U^{(k)}$, $S^{(k)}$ and $V^{(k)}$ are the posture primitive matrix, the significance matrix, and the time modulation matrix respectively, for k number of primitives, J is the matrix of preprocessed joint data profiles, and M is the number of samples recorded in trial i.

Fig. 3(a) shows the distribution of RMS errors over trials for varying number of primitives for each joint. The values have been normalized to the maximum of all trials. By observing the errors, it can be concluded that a good approximation could be obtained by considering two or three primitives only. The maximum error among all trials is 11.6% for two primitives and 9.5% for three primitives (Fig. 3(b)). Those results are in line with the observations of Santello et al. [4].

A comparison between the reconstructed joints and the de-noised data can be observed in Fig. 4(a) and Fig. 4(b) for two and three synergies employed respectively. It can be noted that a higher number of synergies renders a preshaping policy more similar to the original data, especially for some joints.

3) Integration of Different Teaching Trials: This step is illustrated in Fig. 2.C. Since eight demonstration trials have been performed for grasping the same object, the problem of abstracting them to one set of postural primitives and corresponding time modulation vectors has to be solved. We combined the pre-processed joint data matrices of each trial into one single matrix, and we applied SVD decomposition on it. Concatenating joint matrices from different trials poses the problem of separating the contribution of each sequence for extracting common time modulation vectors. We solved this problem of abstraction by performing K-Means clustering [19] of the ensemble of v_i, $i = 1, 2, 3, \cdots, 8$ vectors from the 8 demonstrations as shown in Fig. 5. Centroids of clusters (*milestones*) are used as key points to build interpolating cubic splines to reconstruct an abstracted preshaping policy. We used the longest demonstration as a guide to determine the number of clusters ($K = 7$) of the K-means clustering algorithm. This resulted in a best fit spline per each eigenposture.

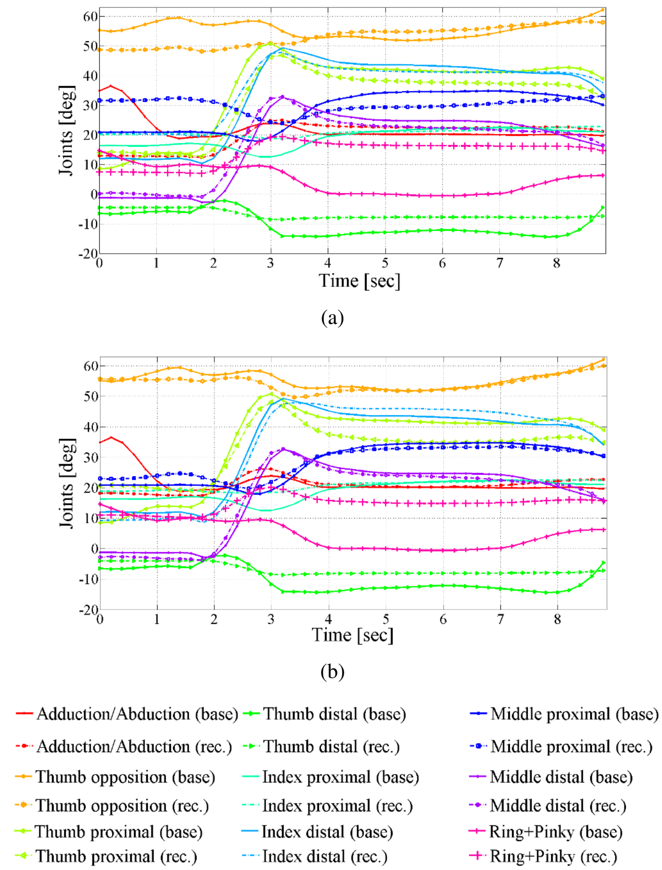

(a)

(b)

Fig. 4. Comparison between de-noised joint values of trial 6 (continuous line) and reconstructed ones (dashed line) using **(a)** two primitives and **(b)** three primitives.

Thank to the orthogonality property of SVD, each component of the v_i matrices can be interpolated separately. It is therefore possible to simplify a 9-dimensional control algorithm to two or three independent spline interpolation problems.

C. Kinematic Multi-fingered Enveloping

The final stage of grasping is the kinematic enveloping. Postural primitives extracted from the SVD analysis and the corresponding spline interpolations of the temporal modula-

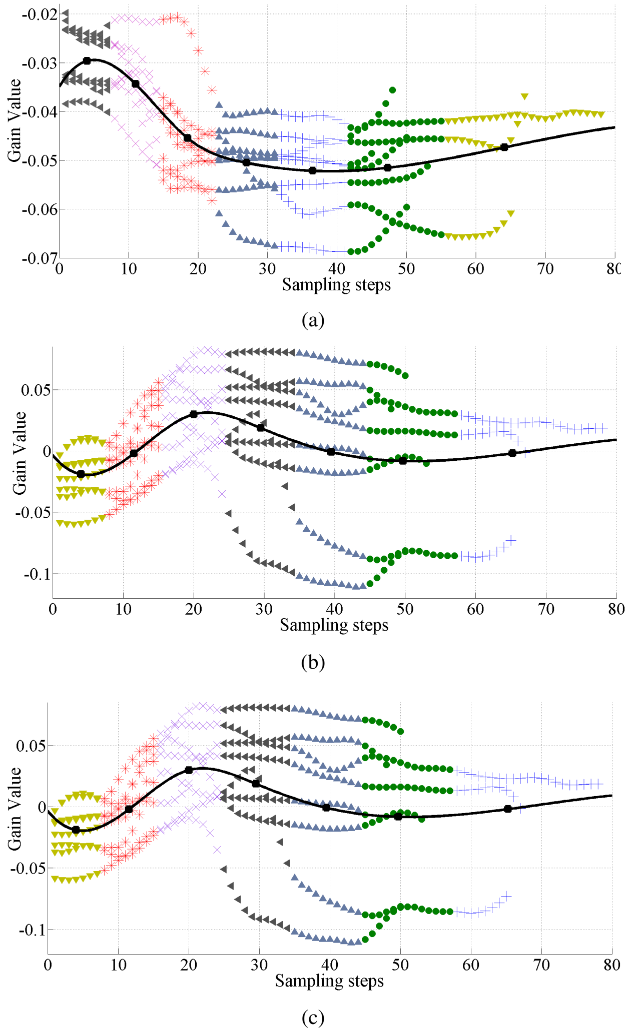

Fig. 5. Results of K-Means clustering on temporal modulation vectors. Vectors v_i 5(a) $i = 1$, 5(b) $i = 2$, 5(c) $i = 3$] from different trials are clustered independently in order to obtain a set of 7 key points for spline interpolation. Cubic Spline interpolation from resulting milestones is shown as black curve for each dimension.

tion coefficients were used to compute the final preshaping grasp policy realtime. This step is summarized in Fig. 2.D.

Once the hand is preshaped by following the joint values encoded in the grasp policy, each finger wraps around the object trying to squeeze it. We used joint encoder readings collected over a given time horizon ($t_f = 10$ sec) to detect the success of a grasping sequence. This enhances the portability of the algorithm to different robotic platforms that may or may not have tactile feedback on the fingertips.

A digit is considered to be steady if:

$$d_i \in [f_i(l) | h_i < x_f] \tag{3}$$

Where d_i is the total angular displacement of digit i, f_i is the function regulating the motion of joint i, k is the current number of encoder data samples, h_i is the total angular displacement of the i-th joint in a given time horizon ($t_f = 10$ sec), x_f is the threshold total angular displacement to detect whether a significant angular displacement has occurred in each time horizon.

The execution flow is resumed in algorithm 1. $c_i = 2.5°$

Algorithm 1: Kinematic Enveloping Algorithm

Data:
- t - execution time $[0 \cdots \infty)$ sec
- h_i - total displacement of joint i
- f_i - motion of joint i
- l - number of iterations of the algorithm
- x_f - threshold defining if the motion of a joint is negligible
- c_i - constant increment of joint i
- T - sampling time
- t_f - temporal horizon when stopping criteria is evaluated
- P - number of joints whose motion has been detected as negligible
- $Jlim_i$ - limit for joint i

begin
  $P = 0$;
  for $l = \lceil \frac{t}{T} \rceil; f_i < Jlim_i$ **do**
    for $i = [1 \cdots J_n]$ **do**
      $f_i(l) = lc_i$;
      $h_i(l) = \sum_{q=0}^{q=l} f_i(q)$;
      if $l = \lceil \frac{t_f}{T} \rceil$ **and** $h_i(l) < x_f$ **then**
        $P = P + 1$;
      end
      if $P >= 6$ **then**
        return *true* `// Grasp successful`
      end
    end
  end
  return *false* `// Grasp unsuccessful`
end

is the amount of angular increment of i-th joint in each sampling step $T = 1.6$ sec. The increment c_i has been selected from the mechanical constraints of the robot to ensure an observable motion due to the resolution of the encoders. The time horizon t_s to detect a terminal condition, is set to 10 seconds, while x_f is set to $10°$. The time horizon t_f and the threshold x_f are the functions of the increment and have been derived from tests on different objects. If the number of stationary joints $P >= 6$ the object is considered grasped. This number has been evaluated experimentally, based on the assumption that at least three digits are needed to grasp tightly [20] and that about two joints are controlling a single finger. The quality of the grip is validated experimentally as illustrated in next section.

III. Experimental Evaluation

In this section, the proposed algorithm is validated on a robot by grasping real-world objects. At first the robotic platform, iCub, is introduced. Secondly, the experimental set-up and the validation criteria are described. Finally, the results of the algorithm are discussed.

Object Name	No. of Synergies	Grade of stability	Duration [sec]	Preshaping time [sec]	Enveloping time [sec]
 Cuboid*	3	4	78	35	43
	2	3	92	37	55
 Cylinder*	3	4	133	30	103
	2	4	89	26	63
	1	3	111	30	81
	Envl. Only	2	119	-	119
 Receiver	3	4	109	73	36
	2	4	109	74	35
	1	2	109	74	35
	Envl. Only	2	56	-	56
 CD Case	3	1	124	74	50
	2	1	120	74	46
	1	1	127	72	55
	Envl. Only	1	48	-	48
 Markers	3	4	119	73	46
	2	3	119	74	45
 Mouse	3	2	116	77	39
	2	2	109	74	35
	1	1	109	74	35
	Envl. Only	0	4	-	4
 Glass	3	0	111	73	38
 Handle	3	3	122	77	45
	Envl. Only	3	59	-	59

TABLE I

Summary of grasping experiments on the set of objects. (*) The time has been evaluated using different parameters for the kinematic enveloping phase ($c_i = 1.0$, $t_c = 0.5$), moreover the termination of the enveloping was manual.

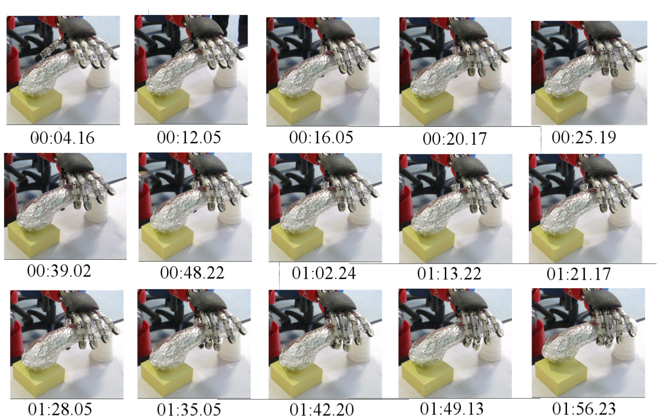

Fig. 6. Evolution of the grasp on the real robot using two primitives for preshaping. The time reported in the first picture takes into account the required computation to start the algorithm. An example of execution can be visualized in the accompanying video.

Index	Description	Median of Force (N)	Standard Deviation of Force (N)
4	The object is removed with a significant effort from the operator, possibly using two hands and manually opening the robot's hand.	92.35	7.23
3	The object is removed with significant effort from the operator but without interacting with the robot's hand.	51.59	5.88
2	The object is removed sliding it from the robot's hand applying discrete effort with no interaction with the robot's hand.	15.81	1.48
1	The object is easily removed with little effort and without interacting with the robot's hand.	4.9	1.86
0	The object is not grasped or is falling while being picked up.	-	-

TABLE II

Description of the ranking score for grip validation. The scores are visually demonstrated in the accompanying video.

A. Description of Robotic Platform

The iCub is a 104 cm tall humanoid robot resembling a 3.5 year old child [21] with 53 degrees of freedom in total - including seven for each arm and nine for each hand. The hands are actuated with a tendon driven system with the motors located in the forearm (Faulhaber 1016M012G). Encoders are based on hall sensors. The hands of the robot are equipped with capacitive pressure sensors [22] that are distributed on palms, fingertips and the rest of the body. Twelve taxels are allocated on the fingertips, and detect the contact with conductive material (such as metal or human skin).

The robot, apart from the interface API that communicates directly to the hardware, is operated through YARP [23], an open-source robotic middleware that supports distributed computation.

B. Experimental Setting

In order to validate the algorithm, several experiments have been carried out with the iCub grasping different objects. The objects used in the experiments are shown Table I. The hand should be positioned at a maximum distance of 5 cm from the grasping point in order to manage a successful grasp.

Afterwards, the algorithm is executed and the preshaping is performed. Then the kinematic enveloping phase takes place. Our technique differs from other methods [24] based on known contact points, therefore the concepts of force/form closure [25] are not an appropriate method to validate the stability of the grip using as the position of the contact points is not known a priori. Instead, validation has been carried out experimentally. Once the algorithm terminates, the object is vertically lifted at about $22 \cdot 10^{-3} m/s^2$ and a human operator pulls the object from the robotic hand to verify the stability of the grip (Table II). Each grip has been ranked based on the force exerted by the human operator, it

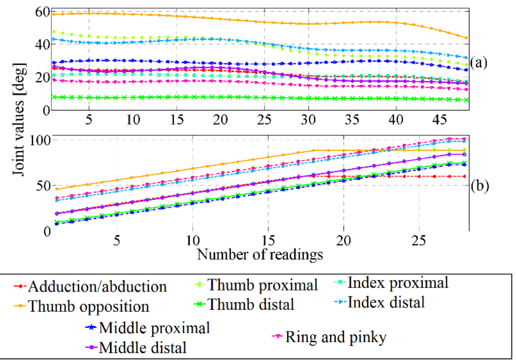

Fig. 7. Evolution of joint values for grasping a telephone receiver using three synergies. **(a)** Evolution of the joints of the hand during the preshape phase. **(b)** Evolution of the joints of the hand during the kinematic enveloping phase. The fingers are closing linearly until the object's surface is hit. Afterwards, the motion reaches a steady state and the grasp termination is detected.

has been estimated experimentally using a 6 DoF force and torque sensor (MINI40, ATI Technologies).

C. Experimental Validation and Discussion

In order to validate the robustness and generalization power of our grasping technique, all objects in the set are grasped with different numbers of synergies: three, two, one or just with the kinematic enveloping.

To analyse whether different demonstrations are able to produce a feasible preshaping policy, despite the variability of the teaching trials, it is possible to observe the evolution of a grasping sequence using just two primitives as in Fig. 6. It can be observed that the conjunction of different demonstrations executed on the same object - the cuboid - produced a stable grasping policy. Thanks to the K-Means clustering and the spline interpolation, it is possible to combine different demonstrations in order to produce a unique preshaping policy.

Fig. 7 shows the reconstructed evolution of the joint angles during the grasp execution, while grasping a telephone receiver using three synergies. As explained in section II-B.3, the preshaping follows a policy defined from the extraction of synergies from kinaesthetic data. Therefore its evolution is very similar across different objects. The enveloping phase, however, differs from object to object. Fig. 6 displays a typical evolution of grasping a telephone receiver has a similar shape to many other objects, such as cuboids and the cylinders. It can be clearly seen that, as defined in section II-C, the joints are linearly closing until the object is enveloped with the fingers reaching a steady state.

Table I summarizes the results of grasping the objects. It can be seen that the telephone receiver, the markers, the cylinder, the cuboid and even a complex shaped fencing handle, are tightly grasped (see grade of stability in the third column of Table I and Table II for the description of grades of stability). The reason is that their geometries are similar to the object used for learning and the thumb is placed on the right position - ranked 4 to 3 on Table I. The computer mouse is grasped but the grip is not tight - ranked 2 on Table I.

The Compact Disc (CD) keep case was not successful since its geometry differs from a standard cuboid and requires a parallel grasp [26]. As the shape of the glass is cylindrical, we were interested in testing a grasp with splayed fingers from the top. However, the grasp was unsuccessful due to the very specific digit configuration required.

Based on the experimental studies, we have found out that misplacement of the yaw angle of the opposition joint of the thumb (angle between the thumb and the index finger) is the cause for most of failures. This conclusion is logical, because this degree of freedom in the primate thumb has given them the skill to manipulate objects [27]. Other digits played a more supportive role role in achieving a good grasp.

The experimental results given in Table I confirm that the difference between three and two postural primitives is negligible. Both design choices perform comparatively well, as the thumb opposition placement is similar. Using only one synergy causes failures due to the very large dimensionality reduction and its consequent reconstruction error. The thumb is often misplaced leading to an unsuccessful grasp.

The enveloping phase has been proved to be very helpful but not sufficient to finalize the grasp. Unless the object geometry is very simple, enveloping only may cause failures due to the blind placement of the thumb on the object. However, with a proper initial configuration of digits after pre-shaping phase, the enveloping helped to generalize even for cases where the size of the object was smaller or the geometry was slightly different from the original object used to demonstrate grasping.

Among the two parts of the algorithm - preshaping and enveloping - it can be seen that the second stage is generally much faster than the first. The reason is that the fingers move quickly and generally the enveloping is executed after preshaping, so the number of iterations cannot be very large. The preshaping phase, instead, is longer since it depends on the number of sensor readings that, in general, can be very large depending on the demonstration.

In the case of the cuboid, the overall time limited, since the list of joints commands is short (about 48). Indeed, due to mechanical constraints on the robot's hand, a brief pause is required between commands (1.5 seconds in our experiments) to enforce the execution of the command. This problem can be easily circumvented by sub-sampling the policy observing the gradient of each joint. If the derivative is not large enough, it can be deduced that the requested motion is too fine to be achieved and that set of joint commands can be skipped in favour of larger values.

IV. Conclusions and Future Work

This paper proposes a novel algorithm for grasping based on synergies computed using the SVD on kinaesthetic teaching data. The 9-dimensional joint space of the hand of the iCub robot can be reduced to two or three postural primitives that can be independently combined thank to the orthogonality property of SVD. Data collected from different trials can be integrated through the use of K-Means clustering and spline interpolation producing a set of time modulated synergies for preshaping the hand. Experiments have shown that the choice between two or three postural primitives does not have a considerable impact on the final quality of the grasp.

To improve the generalization property of the preshaping, the fingers are being wrapped around the object until no significant motion is detected. This phase, called kinematic enveloping, has shown to improve over the preshaping in achieving a more general grip that is able to scale on the target size and geometry of the object. Experimental results show that enveloping in itself is not enough to ensure a safe grip in all cases due to the blind placement of the thumb opposition joint. This joint seems to have a pivotal role on the generalization ability of a set of postural primitives contributing in the preshaping phase.

The significant advantage of the proposed technique relies on the capability of SVD, K-Means clustering and spline interpolation to combine different demonstrations into a unique preshaping policy, regardless of their variability among trials. The kinematic enveloping only strengthen the generalization ability of the preshaping policy by dynamically adapting the fingers to the geometry of the object at hand, and guarantees a stable grasp on objects scaled with respect to the learned one. Moreover, kinaesthetic teaching intrinsically solves the correspondence problem, as the robot learns in its own joints space. Employing this demonstration technique saves from the burden of mapping the human kinematics as in other approaches [7], [14].

In future work we will evaluate the algorithm on different robotic hands in order to test how well the parameters may scale on different kinematics and mechanical designs. Furthermore, the algorithm will be tested on soft objects to evaluate the deformation caused by the present enveloping controller.

V. Acknowledgements

The research leading to these results has received funding from the European Community's Seventh Framework Programme (FP7/2007-2013) project DARWIN (Grant No: FP7-270138). The authors would like to acknowledge the contribution of each DARWIN partner and would like to thank Dalia De Sanctis and Jacopo Zenzeri for their help and support and Raffaello Bonghi for the insightful talks.

References

[1] H. Mellmann and G. Cotugno, "Dynamic motion control: Adaptive bimanual grasping for a humanoid robot," *Fundamenta Informaticae*, vol. 112, no. 1, pp. 89–101, 2011.

[2] M. Santello, M. Flanders, and J. F. Soechting, "Postural hand synergies for tool use," *The Journal of Neuroscience*, vol. 18, no. 23, pp. 10 105–10 115, 1998.

[3] M. Santello, G. Baud-Bovy, and H. Jrntell, "Neural bases of hand synergies," *Frontiers in Computational Neuroscience*, vol. 7, no. 23, 2013.

[4] M. Santello, M. Flanders, and J. F. Soechting, "Patterns of hand motion during grasping and the influence of sensory guidance," *The Journal of Neuroscience*, vol. 22, no. 4, pp. 1426–1435, 2002.

[5] A. Jiang, J. Bimbo, S. Goulder, H. Liu, X. Song, P. Dasgupta, K. Althoefer, and T. Nanayakkara, "Adaptive grip control on an uncertain object," in *Intelligent Robots and Systems (IROS), 2012 IEEE/RSJ International Conference on*, Oct 2012, pp. 1161–1166.

[6] C. Mason, J. Gomez, and T. Ebner, "Hand synergies during reach-to-grasp," *Journal of Neurophysiology*, vol. 86, no. 6, pp. 2896–2910, 2001.

[7] C. Brown and H. Asada, "Inter-finger coordination and postural synergies in robot hands via mechanical implementation of principal components analysis," in *Intelligent Robots and Systems, 2007. IROS 2007. IEEE/RSJ International Conference on*, 2007, pp. 2877–2882.

[8] A. Bicchi, M. Gabiccini, and M. Santello, "Modelling natural and artificial hands with synergies," *Philosophical Transactions of the Royal Society B: Biological Sciences*, vol. 366, no. 1581, pp. 3153–3161, 2011.

[9] G. Grioli, M. Catalano, E. Silvestro, S. Tono, and A. Bicchi, "Adaptive synergies: an approach to the design of under-actuated robotic hands," in *Intelligent Robots and Systems (IROS), 2012 IEEE/RSJ International Conference on*. IEEE, 2012, pp. 1251–1256.

[10] H. Yousef, M. Boukallel, and K. Althoefer, "Tactile sensing for dexterous in-hand manipulation in robotics a review," *Sensors and Actuators A: Physical*, vol. 167, no. 2, pp. 171 – 187, 2011.

[11] K. Althoefer, B. Krekelberg, D. Husmeier, and L. Seneviratne, "Reinforcement learning in a rule-based navigator for robotic manipulators," *Neurocomputing*, vol. 37, no. 14, pp. 51 – 70, 2001.

[12] A. J. Ijspeert, J. Nakanishi, and S. Schaal, "Movement imitation with nonlinear dynamical systems in humanoid robots," in *Robotics and Automation, 2002. Proceedings. ICRA'02. IEEE International Conference on*, vol. 2. IEEE, 2002, pp. 1398–1403.

[13] B. D. Argall, S. Chernova, M. Veloso, and B. Browning, "A survey of robot learning from demonstration," *Robotics and Autonomous Systems*, 2009.

[14] H. Ben Amor, O. Kroemer, U. Hillenbrand, G. Neumann, and J. Peters, "Generalization of human grasping for multi-fingered robot hands," in *Intelligent Robots and Systems (IROS), 2012 IEEE/RSJ International Conference on*. IEEE, 2012, pp. 2043–2050.

[15] C. L. Nehaniv and K. Dautenhahn, "2 the correspondence problem," *Imitation in animals and artifacts*, p. 41, 2002.

[16] V. Klema and A. Laub, "The singular value decomposition: Its computation and some applications," *Automatic Control, IEEE Transactions on*, vol. 25, no. 2, pp. 164–176, 1980.

[17] V. Mohan and P. Morasso, "Passive motion paradigm: an alternative to optimal control," *Frontiers in Neurorobotics*, vol. 5, no. 4, 2011.

[18] A. Savitzky and M. J. E. Golay, "Smoothing and Differentiation of Data by Simplified Least Squares Procedures," *Analytical Chemistry*, vol. 36, 1964.

[19] J. B. MacQueen, "Some methods for classification and analysis of multivariate observations," in *Proc. of the fifth Berkeley Symposium on Mathematical Statistics and Probability*, L. M. L. Cam and J. Neyman, Eds., vol. 1. University of California Press, 1967, pp. 281–297.

[20] E. Chinellato, R. Fisher, A. Morales, and A. Del Pobil, "Ranking planar grasp configurations for a three-finger hand," in *Robotics and Automation, 2003. Proceedings. ICRA '03. IEEE International Conference on*, vol. 1, 2003, pp. 1133–1138 vol.1.

[21] G. Metta, L. Natale, F. Nori, G. Sandini, D. Vernon, L. Fadiga, C. von Hofsten, K. Rosander, M. Lopes, J. Santos-Victor, A. Bernardino, and L. Montesano, "The icub humanoid robot: An open-systems platform for research in cognitive development," *Neural Networks*, vol. 23, no. 8-9, pp. 1125–1134, 2010.

[22] G. Cannata, M. Maggiali, G. Metta, and G. Sandini, "An embedded artificial skin for humanoid robots," in *Multisensor Fusion and Integration for Intelligent Systems, 2008. MFI 2008. IEEE International Conference on*, 2008, pp. 434 –438.

[23] P. Fitzpatrick, G. Metta, and L. Natale, "Towards long-lived robot genes," *Robot. Auton. Syst.*, vol. 56, no. 1, pp. 29–45, 2008.

[24] B. Siciliano and O. Khatib, *Springer handbook of robotics*. Springer, 2008.

[25] A. Bicchi and V. Kumar, "Robotic grasping and contact: A review," in *Robotics and Automation, 2000. Proceedings. ICRA'00. IEEE International Conference on*, vol. 1. IEEE, 2000, pp. 348–353.

[26] T. Feix, R. Pawlik, H. Schmiedmayer, J. Romero, and D. Kragic, "A comprehensive grasp taxonomy," in *Robotics, Science and Systems: Workshop on Understanding the Human Hand for Advancing Robotic Manipulation*, June 2009.

[27] M. W. Marzke and K. L. Wullstein, "Chimpanzee and human grips: A new classification with a focus on evolutionary morphology," *International Journal of Primatology*, vol. 17, no. 1, pp. 117–139, 1996.